Adhesion of solids

Maxim Vergeles,[1] Amos Maritan,[2] Joel Koplik,[3] and Jayanth R. Banavar[1]
[1]*Department of Physics and Center for Materials Physics, The Pennsylvania State University, 104 Davey Laboratory, University Park, Pennsylvania 16802*
[2]*International School for Advanced Studies (SISSA), Via Beirut 2-4, 34014 Trieste, Italy*
[3]*Benjamin Levich Institute and Department of Physics, City College of New York, New York, New York 10031*
(Received 24 April 1997)

We report results of studies of adhesion of two solids on a microscopic level. We show that the Johnson-Kendall-Roberts theory [Proc. R. Soc. London A **324**, 301 (1971)] remains valid even at this level, and that the effects of roughness and an intervening fluid can be accounted for by adjusting the value of the work of adhesion. We study adhesion hysteresis and demonstrate that, in our system, it arises from bulk effects. We also find that the detachment of spherical particles from solid surfaces occurs at smaller values of the shear rate than predicted by continuum theory, due to slip between the particle and the solid surface which is not taken into account by continuum theories. [S1063-651X(97)03409-0]

PACS number(s): 64.60.Ht, 68.70.+w, 92.40.Fb, 92.40.Gc

I. INTRODUCTION

The problem of the behavior of two spheres or a sphere and a plane pressed against each other (Fig. 1) has a long history. The earliest study is due to Hertz, who solved the problem by assuming that adhesion forces between the two surfaces were negligible [1]. He showed that the radius of the contact area is $a=(RF/K)^{1/3}$ and that the central displacement is $\delta=a^2/R$, where $R=R_1R_2/(R_1+R_2)$, $K=\frac{3}{4}[(1-\sigma_1^2)/E_1+(1-\sigma_2^2)/E_2]$, $R_{1,2}$, $\sigma_{1,2}$, and $E_{1,2}$ are the radii, the Poisson's ratios, and the Young's moduli for the two spheres, and F is an applied load. In 1971, Johnson, Kendall, and Roberts (JKR) [2] improved the Hertz theory by incorporating the effects of adhesion through the requirement of energy minimization. The JKR theory predicts that

$$a^3=\frac{R}{K}\left[F+3\pi RW+\sqrt{6\pi RWF+(3\pi RW)^2}\right], \tag{1}$$

$$\delta=\frac{a^2}{R}\left[1-\frac{2}{3}\left(\frac{a_0}{a}\right)^{3/2}\right] \tag{2}$$

and the pressure within the contact area is

$$P(r)=\frac{3Ka}{2\pi R}[1-(r/a)^2]^{1/2}-\left(\frac{3KW}{2\pi a}\right)^{1/2}[1-(r/a)^2]^{-1/2}, \tag{3}$$

where r is the radial coordinate in the contact plane (see Fig. 1), W is the surface energy per unit area, and $a_0=(6\pi R^2W/K)^{1/3}$ is the contact radius under zero load ($F=0$).

One of the drawbacks of the JKR analysis is that it predicts an infinite stress at the edge of the contact area [the second term on the right-hand side of Eq. (3)]. This problem arises because the JKR theory is a continuum theory that implicitly assumes that the molecular forces act over infinitesimally small distances. If one takes into account the finite range of molecular forces, assuming, for example, a Lennard-Jones potential for them, the singularity is removed [3]. Apart from its breakdown within the few angstroms from the edge of the contact area, the JKR theory has been shown to describe experimental results for molecularly smooth surfaces on a macroscopic scale quite well [2,4,5].

However, there are very few studies of adhesion on a microscopic scale. Except for the pioneering work of Landman and co-workers [6], who studied tip-substrate interactions in an atomic-force microscope, and Thompson and Robbins [7], who were interested in the stick-slip motion of two solid surfaces separated by thin layer of fluid, most approaches to this problem are based on continuum mechanics. At the same time, the problem of what happens on a molecular scale when two solid bodies are pressed into contact has become even more important recently due to rapidly growing interest in nanotechnology.

Another limitation of the JKR theory is its assumption of absolutely smooth surfaces. In reality, most particles are rough, and it is well known that even small asperities can have a significant effect on adhesion. Also, the JKR theory does not describe important situations such as the mechanical contact of two solid bodies in the presence of an intervening fluid.

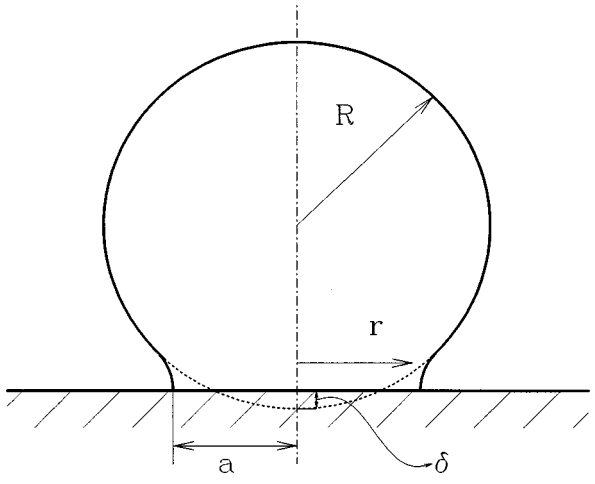

FIG. 1. A sketch of a sphere pressed against a planar surface.

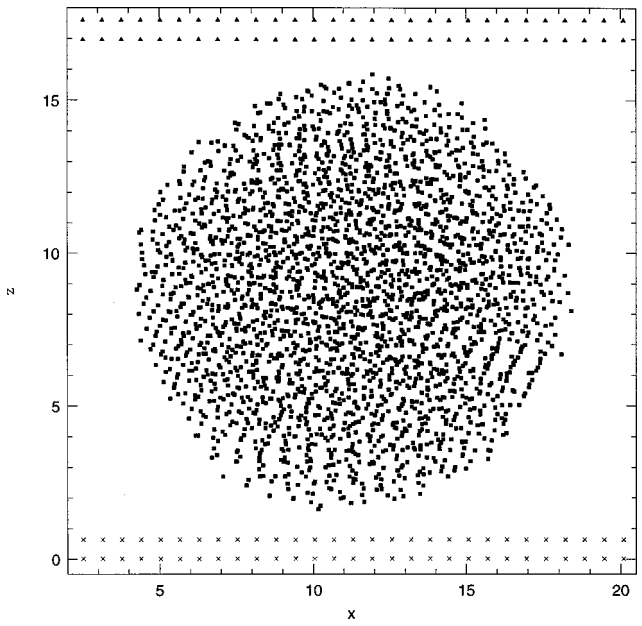

FIG. 2. A snapshot of the initial molecular configuration for the MD simulations of adhesion.

In this work, we use molecular dynamics (MD) simulations to study adhesion of spherical particles, at the molecular level, on smooth and rough surfaces, with and without an intervening fluid. Our results show that the JKR theory works well for smooth surfaces even when the size of the adhering particles is comparable with that of individual molecules. We also show that the effects of roughness and an intervening fluid can be accounted for by an effective value of the surface energy W, which depends on the configuration of the two solids and the fluid. We study the hysteresis associated with the adhesion of solids and find that in our system it is due to bulk effects. We conclude with a study of the detachment of solid particles from solid surfaces, an interesting and important technological problem, which is closely related to the adhesion of solids.

II. MOLECULAR DYNAMICS

We have used a standard MD algorithm in which molecules interact via a pairwise Lennard-Jones potential:

$$V_{ij}(r)=4\epsilon\left[D_{ij}\left(\frac{r}{\sigma}\right)^{-12}-C_{ij}\left(\frac{r}{\sigma}\right)^{-6}\right]. \tag{4}$$

The natural time unit is given by $\tau=\sigma\sqrt{(m/\epsilon)}$, where m is the molecular mass. In the remainder of this paper all dimensional quantities given as pure numbers will be understood as multiplied by an appropriate combination of σ, ϵ, and m. The coefficients C and D in Eq. (4) are used to tune the strength of interaction between molecules of different species.

In our simulations, Newton's equations of motion were integrated using a fifth order predictor-corrector algorithm with a time step of 0.0025τ. A layered-linked cell algorithm [8] was implemented to speed up the computation. The geometry of our simulations is shown in Fig. 2—a spherical ball is squeezed by two solid walls, giving two adhesive contacts. The wall molecules were arranged in an fcc lattice with a lattice parameter of 1.26σ, their mass was chosen to be very large (10^8), so that the Young's modulus of the walls $E_w=\infty$ and $K=\frac{3}{4}[(1-\sigma_b^2)/E_b]$. In our simulations we used a ball of radius $R=7.12$, consisting of 14^3 individual molecules, which did not possess any long-range order. To obtain this ball, we started with the molecules arranged in a simple cubic lattice, and switched off the attraction between them for 1.25τ, allowing the ball to expand and lose its lattice structure in the process. After 1.25τ we switched the attraction on, and the ball molecules coalesced together to form the ball used in our simulations. If instead one uses a ball in which the molecules are arranged in a lattice with long range order, as one compresses the ball one observes huge jumps in the values of the force acting on it. The jumps occur each time the number of molecular layers in the ball decreases by one and the ball undergoes structural changes.

The coefficients C and D in Eq. (4) were $C_{bb}=8.0$, $D_{bb}=1.25$ for the interaction between the ball molecules and $C_{bw}=D_{bw}=5.0$ for the interaction between the ball and wall molecules. Our specific choice of C and D is not important—we have verified that our results are not sensitive to small changes in C and D. To determine the surface energy per unit area W, we cut our ball into two halves by a horizontal plane passing through its center, took just the upper half and measured the energy of the interaction between the molecules of the bottom wall and the molecules of the half ball as a function of the separation between the bottom wall and the half ball. (This geometry was used in order to obtain a planar contact area). W is given by the minimum interaction energy divided by πR^2, where R is the ball radius. This procedure gives $W=13.0$. Alternatively, one may assume that the $z<0$ region of space is filled with a jellium of uniform density corresponding to that of the wall molecules, while the $z>d$ region of space is occupied by a jellium of the ball molecules. One may then integrate the interactions between them to obtain the energy of interaction per unit area as a function of d. W is given by the maximum attractive interaction energy. This method yields $W=13.2$, which is quite close to the previous value of 13.0. The temperature T was chosen to be 1.0. At this temperature the ball was in the solid phase with values of E_b and σ_b, yielding $K=264.4$. To obtain the values of E_b and σ_b, we imposed a small uniform deformation on the ball and used Hooke's law [9]:

$$\sigma_{ik}=(\lambda+2/3\mu)u_{ll}\delta_{ik}+2\mu(u_{ik}-1/3u_{ll}\delta_{ik}), \tag{5}$$

where σ_{ik} is the stress tensor, u_i is the displacement vector, $u_{ik}=\frac{1}{2}(\partial u_i/\partial x_k+\partial u_k/\partial x_i)$ is the strain tensor, and λ and μ are the Lame coefficients with $E_b=\mu(3\lambda+2\mu)/(\lambda+\mu)$ and $\sigma_b=(\lambda/2)/(\lambda+\mu)$. If the deformation is such that the strain tensor is uniform, then the stress tensor, being linearly related to the strain tensor, is also uniform, and thus equal to its average value [9]:

$$\sigma_{ij}=\langle\sigma_{ij}\rangle=\frac{1}{V}\oint\frac{x_iF_j}{R}\,dA, \tag{6}$$

where the integration is over the surface of the ball, V is the ball volume, x_i is the ith coordinate of the element of the ball surface, and F_j is the jth component of the force acting on

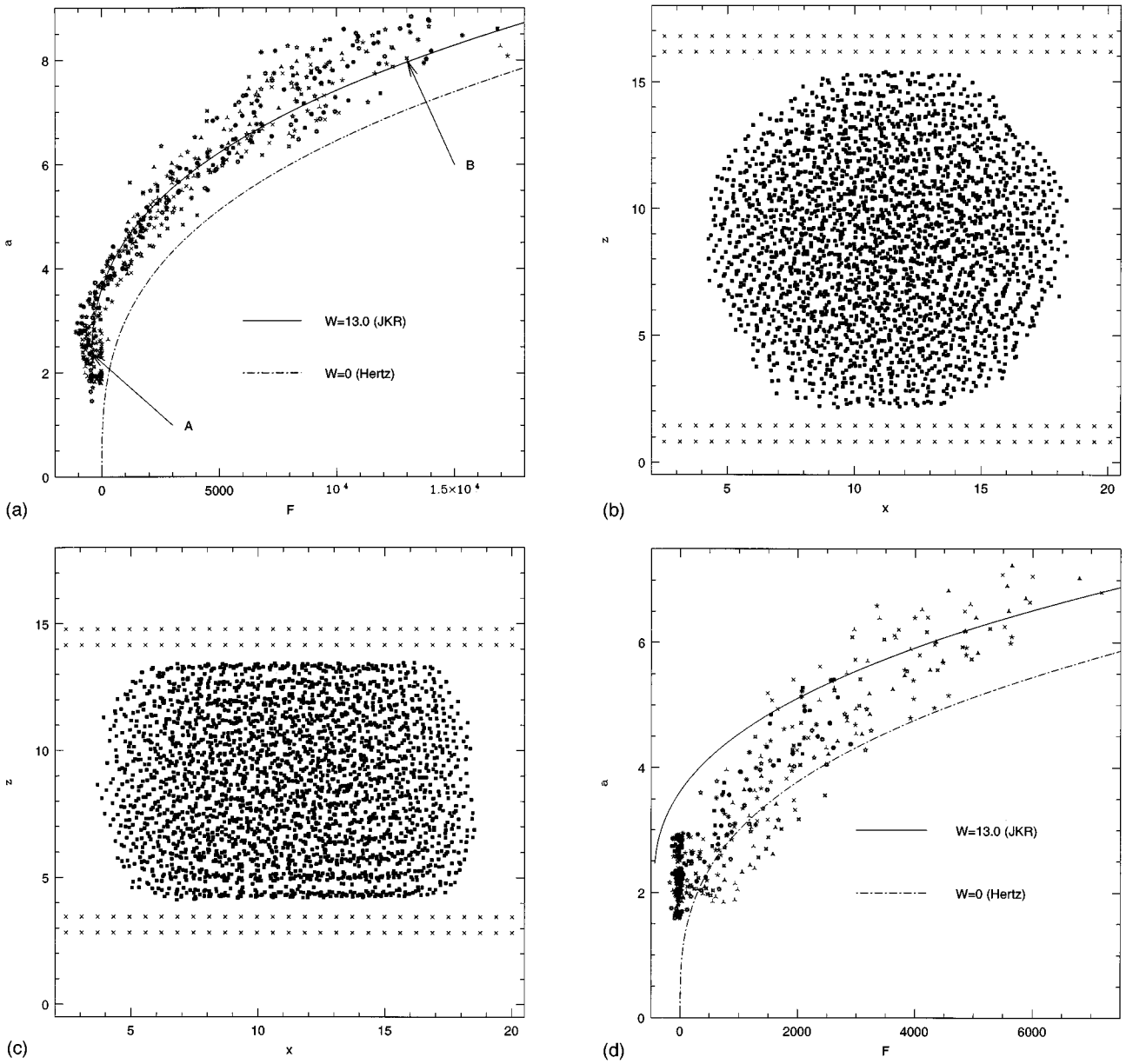

FIG. 3. (a) Radius of contact area a vs applied force F for the smooth wall. Different symbols represent results obtained in four independent runs with two independent adhesive contacts in each run. Solid line represents JKR prediction with $W=13.0$, dashed lines represents Hertz prediction $(W=0)$. (b) A snapshot of the molecular configuration corresponding to point A in (a). (c) A snapshot of the molecular configuration corresponding to point B in (a). (d) Radius of contact area a vs applied force F for the smooth wall with a fluid layer on top of it. Different symbols represent results obtained in four independent runs with two independent adhesive contacts in each run. Solid line represents JKR prediction with $W=13.0$, dashed lines represents Hertz prediction $(W=0)$.

this element. The first term in Eq. (5) corresponds to pure compression and the second term corresponds to pure shear. Thus, by imposing separately compression and shear, and using Eq. (6) to calculate the stress tensor, one can obtain the values of λ and μ, from which it is straightforward to calculate E_b, σ_b, and K.

III. ADHESION

We begin by assessing how well the JKR theory describes adhesion of smooth surfaces on a microscopic scale. To our knowledge, this is the first study of its kind.

Initially, the two walls were placed far apart, and the ball was equilibrated for 25τ. After the ball was equilibrated we fixed the positions of 287 molecules in the middle section of the ball, whose z coordinates were within 0.5σ of the center of mass of the ball, and started moving the walls symmetrically towards the center of the ball. Each wall was moved by 0.1σ during a time interval of 0.5τ and then the system was allowed to relax for 0.25τ. To ensure that the system was fully equilibrated, we performed some runs in which the system was allowed to relax for 0.5τ instead of 0.25τ, and we found that the results were not affected by this change. Over the next 0.5τ, we measured the force F acting on the ball from each wall, the central displacement δ and the radii of both contact areas a (see Fig. 1), after which the whole cycle

was repeated again. The wall induces layering of the ball molecules with the z coordinates of the molecules forming the first layer within 0.5σ of the lowest molecule. In order to calculate the radius of the lower contact area, we identified the lowest ball molecule (the molecule that had the smallest z coordinate $z_{\min}$), considered all ball molecules with z coordinates between $z_{\min}$ and $z_{\min}+0.5\sigma$, projected them on the x-y plane, and calculated the effective radius a, using the expression (designed to yield the correct radius for a circular geometry)

$$a^2/2=\frac{\sum_i [(x_i-x_c)^2+(y_i-y_c)^2]}{N}.$$

Here the sum is over all ball molecules with z coordinates between $z_{\min}$ and $z_{\min}+0.5\sigma$, N is the number of these molecules, x_c and y_c are the x and y coordinates of the center of mass of the group of these molecules. To determine the central displacement δ, we used two methods. The first considered the position of the lowest ball molecule; since the center of the ball does not move in our simulations, δ is given by the current z coordinate of the lowest ball molecule minus the initial position of this molecule. The second method links δ to the position of the wall. Here one assumes that δ is given by the z coordinate of the upper layer of wall molecules plus a constant, which was chosen optimally to produce the best fit. Although the two methods lead to similar results, they are both not very reliable, especially when δ is small: the first method relies on the position of a single molecule, while the second does not depend on the details of the configuration of the ball molecules. Figure 3(a) shows the radius of contact area a versus the applied load F; the solid line is the JKR prediction, the dotted line corresponds to the Hertz theory, and the data points represent the MD results obtained in four independent runs. Figures 3(b) and 3(c) show snapshots of our system, corresponding to points A and B on Fig. 3(a). The JKR theory describes our results quite well. We note here that we were unable to study the decompression of the ball using this method—the relaxation time of the ball during decompression was longer than the duration of our simulations. In order to study adhesion hysteresis we employed a different technique described in the following section.

Next, we put a wetting, one-molecule-thick layer of a fluid on each of the walls. The interaction coefficients for the fluid molecules in Eq. (4) were $D_{ff}=C_{ff}=1.0$, $D_{fb}=C_{fb}=1.0$, and $D_{fw}=C_{fw}=2.0$. The attraction between the wall and the fluid molecules was strong enough to prevent a significant fraction of the fluid molecules from evaporating. Figure 3(d) shows a versus F for this case. One may interpret the result as showing two distinct regimes; at small applied loads F, the MD data follow the Hertz theory, while at large values of F they are well described by the JKR theory. This behavior can be explained by the fact that the Hertz theory is the $W=0$ limit of the JKR theory. The effective work of adhesion, $W=2.0$, in the presence of the intervening fluid is about 15% of the work of adhesion without the fluid. At small values of F, the ball molecules interact mainly with the fluid molecules and because of that the effective work of adhesion W is much smaller than for the ball-wall interaction

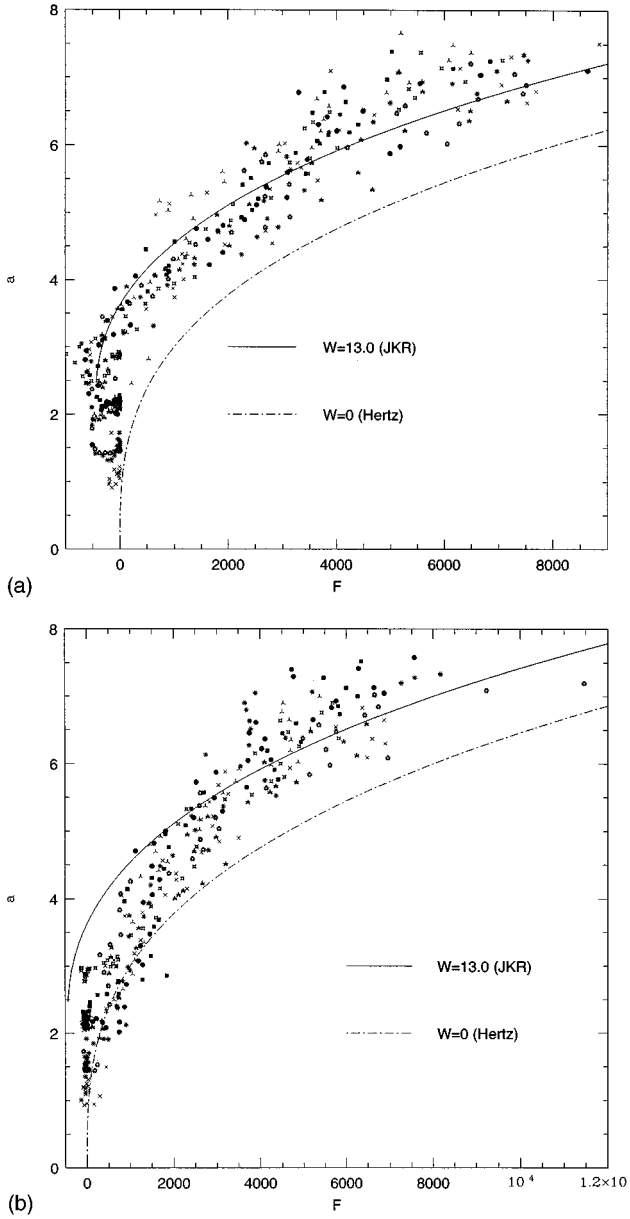

FIG. 4. (a) Radius of contact area a vs applied force F for the rough wall. Different symbols represent results obtained in four independent runs with two independent adhesive contacts in each run. Solid line represents JKR prediction with $W=13.0$, dashed lines represents Hertz prediction ($W=0$). (b) Radius of contact area a vs applied force F for the rough wall with a fluid layer on top of it. Different symbols represent results obtained in four independent runs with two independent adhesive contacts in each run. Solid line represents JKR prediction with $W=13.0$, dashed lines represents Hertz prediction ($W=0$).

and the data are described by the Hertz theory. As the applied load F is increased, the fluid is squeezed from the contact region, and the ball molecules begin to ''feel'' the wall molecules, thus increasing W and switching to the JKR regime.

We also considered the effects of roughness. We put additional wall molecules on each wall with random choices for their x and y coordinates and a z displacement of 1.26σ (equal to the wall lattice parameter) from the crystalline wall. Figure 4(a) shows a versus F for this case. One can see that

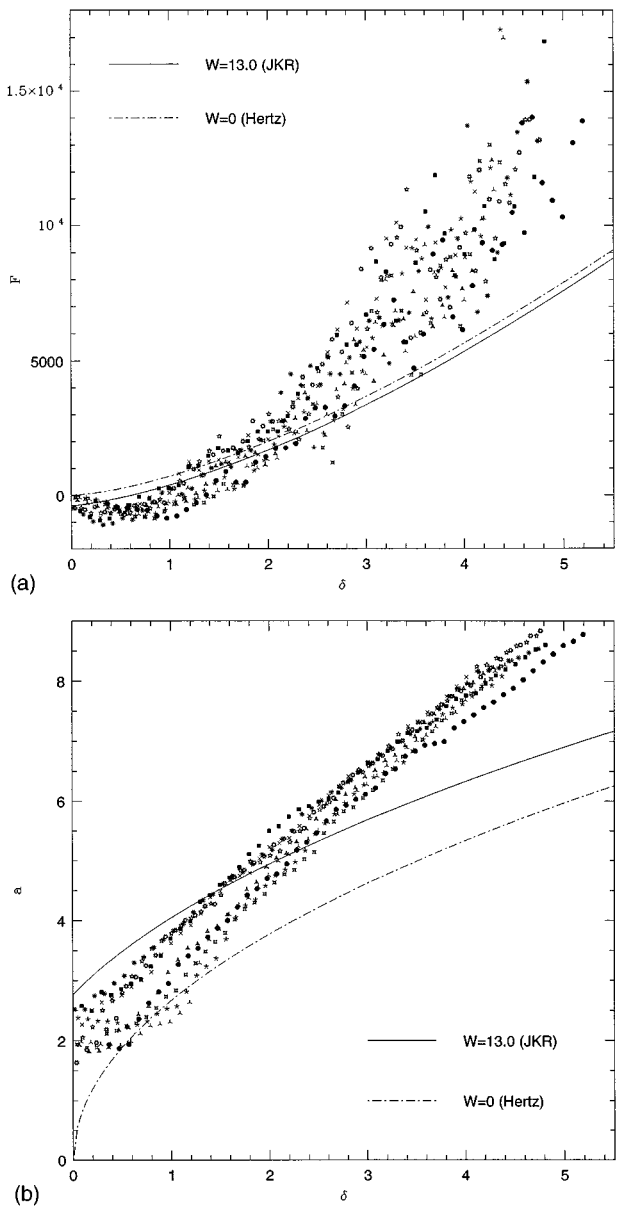

FIG. 5. (a) Applied force F vs central displacement δ for the smooth wall. Different symbols represent results obtained in four independent runs with two independent adhesive contacts in each run. Solid line represents JKR prediction with $W=13.0$, dashed lines represents Hertz prediction $(W=0)$. (b) Radius of contact area a vs central displacement for δ for the smooth wall. Different symbols represent results obtained in four independent runs with two independent adhesive contacts in each run. Solid line represents JKR prediction with $W=13.0$, dashed lines represents Hertz prediction $(W=0)$.

the curve is shifted down with respect to the curve for the smooth surface, which follows from a decrease in the effective work of adhesion W. It is hard to obtain the exact value of the work of adhesion for rough surfaces, but it is clear that it should be smaller than that for smooth surfaces. Figure 4(b) shows a versus F for the case of the rough surface with an intervening fluid, which has the same parameters as before. Again, one can see two different regimes corresponding to low and high values of F.

To conclude this section, we also note that the JKR (or Hertz) theory predicts higher values of the central displacement δ than obtained in our simulations for the same values of applied force F or contact area (Fig. 5). Even though the numerical values of a and F for small δ are necessarily approximately in accord with expectations, the overall trend does not agree with theory. These discrepancies are probably due to the difficulty in extracting a reliable value of δ from our measurements.

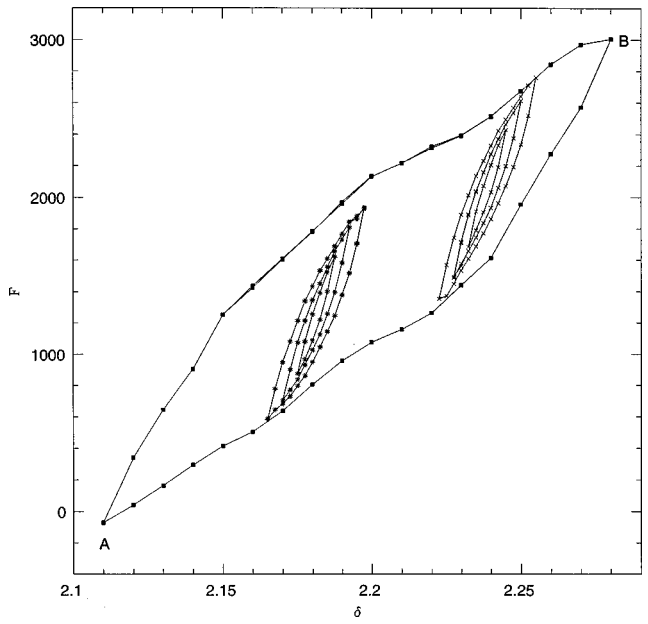

FIG. 6. Applied force F as a function of central displacement δ showing pronounced hysteresis loops.

IV. ADHESION HYSTERESIS

The phenomenon of hysteresis is encountered in many different contexts, such as magnetism, fluid flow, and mechanics [10]. Recent research [11,12] has shown that capillary condensation in porous media and domain dynamics in spin systems exhibit return-point hysteresis. Return-point hysteresis is often described by the Preisach model [13], in which the system is assumed to be made up of independent elementary hysteresis domains. It is well known that adhesion is also associated with hysteresis [3]. The origins of adhesion hysteresis may be traced to processes on the surfaces of the solids or they can arise from bulk dissipation [14].

To study hysteresis in our system, we employed a method of energy minimization, because the MD technique is impractical due to the very long relaxation time of the ball during decompression. We took the ball, described in the previous section, and let it relax, allowing each molecule to move to a position corresponding to a local energy minimum. During this process the walls were placed far away from the ball. The walls, used by us in this study, were smooth 3-9 walls. They interacted with the molecules comprising the ball via a 3-9 potential in the z direction:

$$V(z)=4\epsilon(D_s z^{-9}-C_s z^{-3}),$$

where D_s and C_s were chosen so that the work of adhesion W for these walls was the same as for the molecular walls of the previous section.

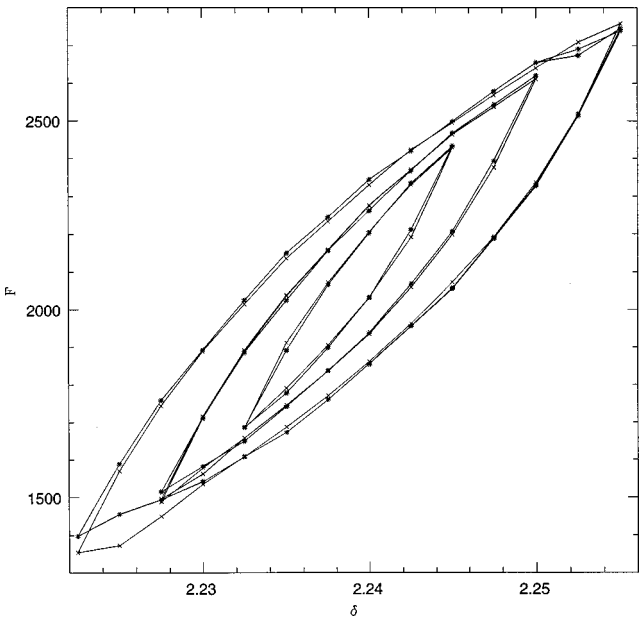

FIG. 7. Two sets of hysteresis loops from Fig. 6 placed on top of each other.

After the ball molecules reached a local energy minimum, we moved the walls towards the ball in small incremental steps. After each step, the system (the ball and the walls) was relaxed into a local energy minimum. We measured the forces acting on the ball from the walls, the radii of the contact areas and the central displacement in the configuration corresponding to this energy minimum. To study hysteresis in our system, we first moved the walls towards the ball in steps of 0.01σ steps and then away from the center of the ball. After cycling several times back and forth within a certain range of values of δ, the system started to move reproducibly along the same loop in the δ-F plane. Figure 6 shows that there is a pronounced hysteresis: the force F is higher during the compression of the ball than during the decompression at the same values of the central displacement δ.

Unlike systems considered in [11,12], our system does not exhibit return-point hysteresis. Hysteresis loops are determined only by the range of change of the central displacement δ and they are substantially unaffected by the previous history of the system (Fig. 6). To obtain this figure we started with the system moving along the big loop between points A and B, then we limited the range of change of δ. On repeated cycling, the trajectory of the system in the δ-F plane evolves until it finally moves reproducibly along a smaller loop between the chosen end points. (In systems exhibiting return-point hysteresis, there is no such evolution). The final loop was the same, independent of whether we were on the upper or lower branch of the A-B-A loop when we reduced the range of change in δ. Return-point hysteresis implies that the system possesses a memory: ''the state of the system can remember an entire hierarchy of turning points in its past external field'' [11]. This ability to remember previous history arises from the existence of certain attributes of the system that are quenched variables: the random local fields in the magnetic systems [11] and the configuration of the porous media in the capillary condensation measurements [12]. In our case, however, the ball molecules move around to accommodate the increasing pressure without any constraints. Thus, unlike the systems described in [11,12], our ball does not have any memory about its past history. The molecules comprising the ball are in local equilibrium within the free energy minimum that the system resides in.

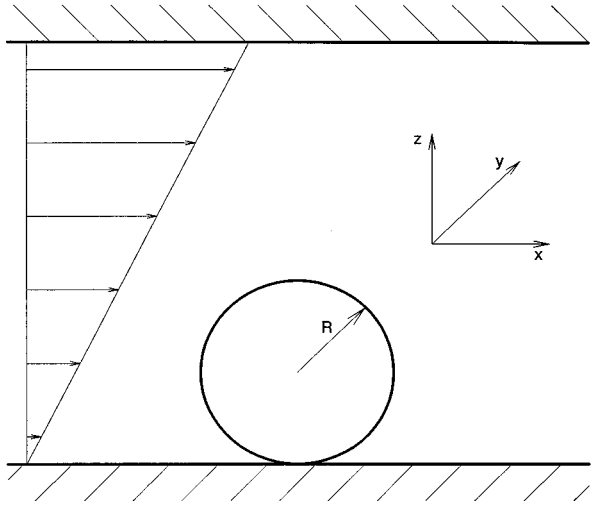

FIG. 8. Detachment of a solid spherical particle from a solid surface.

Figure 7 shows that two sets of loops centered around different values of δ placed on top of each other. They have almost an identical shape. Since the contact areas are quite different for these sets of loops, it is strongly suggestive that in our system the hysteresis is due to bulk dissipation and not due to surface effects.

V. DETACHMENT OF SPHERICAL PARTICLES DUE TO SHEAR FLOW

The problem of detachment of solid particles from solid surfaces is closely related to the adhesion of solids [15]. Previous studies of this problem have identified three possible mechanisms for detachment: rolling, lifting, and sliding [15]. In recent work, [16] King and Leighton have carried out studies of the detachment of spherical particles due to shear flow. They assumed that the detaching particle is rough and that the adhesion forces are negligible. Under these assumptions they calculated translational and rotational velocities of the detaching particle. However, their results do not apply to the case considered here of molecularly smooth particles with a large work of adhesion.

To study this problem we used the following geometry (Fig. 8): we took two parallel walls, filled the space between them with a fluid, and put a ball on one of the walls. Initially the ball was placed near the bottom wall and the system was allowed to equilibrate. In this study we used a ball of radius of 3.5, consisting of 324 molecules. The molecules comprising the ball do not possess any long-range order. The ambient fluid had a density $\rho=0.8$ and a temperature $T=1.2$.

In order to study the role of wall corrugation, we considered a wall that was a combination of a smooth 3-9 wall and a molecular wall, described before. The potential with which the wall interacted with other particles had the form

$$V(r)=4\epsilon\left[b_s(D_s z^{-9}-C_s z^{-3})+b_m\sum\ (D_m r^{-12}-C_m r^{-6})\right],$$

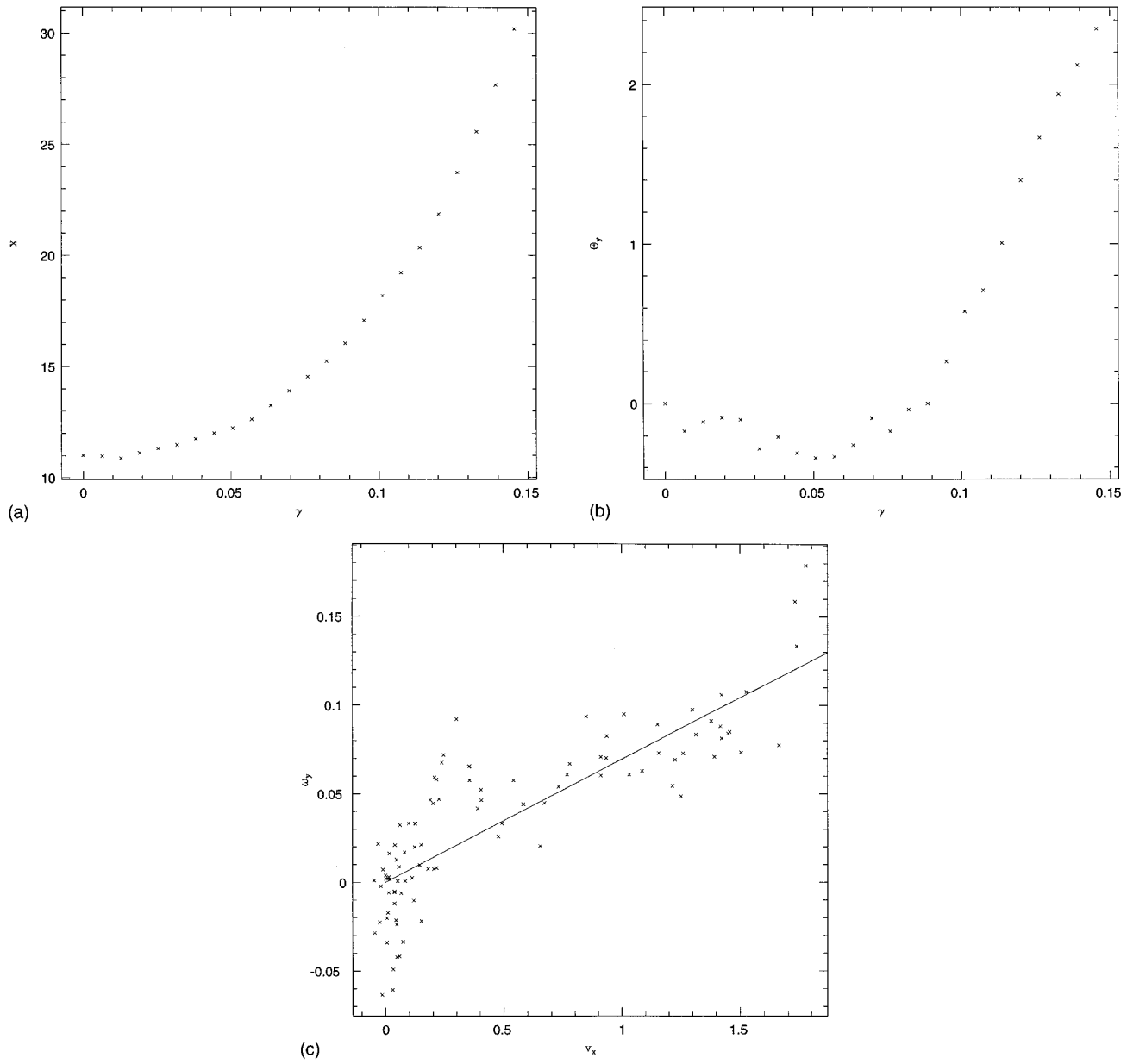

FIG. 9. (a) The x coordinate of the center of mass of the ball as a function of the applied shear rate γ. $b_m=1$, $b_s=0$. (b) The angle of rotation of the ball about y axis as a function of the applied shear rate γ. $b_m=1$, $b_s=0$. (c) The angular velocity of the ball vs the linear velocity of the ball. The solid line represents a linear fit. $b_m=1$, $b_s=0$.

where the sum is over all wall molecules, b_s and b_m are the relative weights of the 3-9 and 6-12 potentials with the constraint $b_s+b_m=1$ to ensure a constant work of adhesion W, again equal to 13.0. $b_m=0$ corresponds to a wall, which is absolutely smooth in the x-y plane, and $b_s=0$ to a significantly corrugated wall.

We equilibrated the system for 25τ, and then we applied shear to our system by setting the upper wall in motion in the x direction. We also divided our system into 50 horizontal bins and rescaled the x velocities of the fluid molecules in each bin, so that the velocity of the center of mass of the bin was $\gamma(z_i-z_b)$, where z_i is the z coordinate of the fluid molecule, z_b is the z coordinate of the bottom wall, and γ is the shear rate. In principle, it is possible to shear the fluid just by setting the upper wall in motion, without rescaling the x velocities of the fluid molecules. However, our method leads to essentially the same results using a much smaller amount of computer time. The shear rate was increased at a rate of $2.5\times10^{-3}\tau^{-2}$. To check that our results do not depend on the rate of γ increase, we let the ball sit on the wall at a value of γ slightly below the detachment threshold for a long time and found that the ball motion in the x direction was diffusive, similar to that under zero shear rate.

Figure 9(a) shows the x coordinate of the center of the ball as a function of the applied shear rate γ for the case of a purely molecular wall ($b_m=1$). Figure 9(b) shows the angle of rotation of the ball about the y axis as a function of γ. The figure demonstrates that in this case the mechanism of detachment is a mixture of rolling and sliding. The ball is translating and rotating at the same time. Figure 9(c) shows angular velocity of the ball as a function of its linear velocity. The linear fit of the form $\omega=v/r_{\text{eff}}$, gives $r_{\text{eff}}=14.4\pm1.4$,

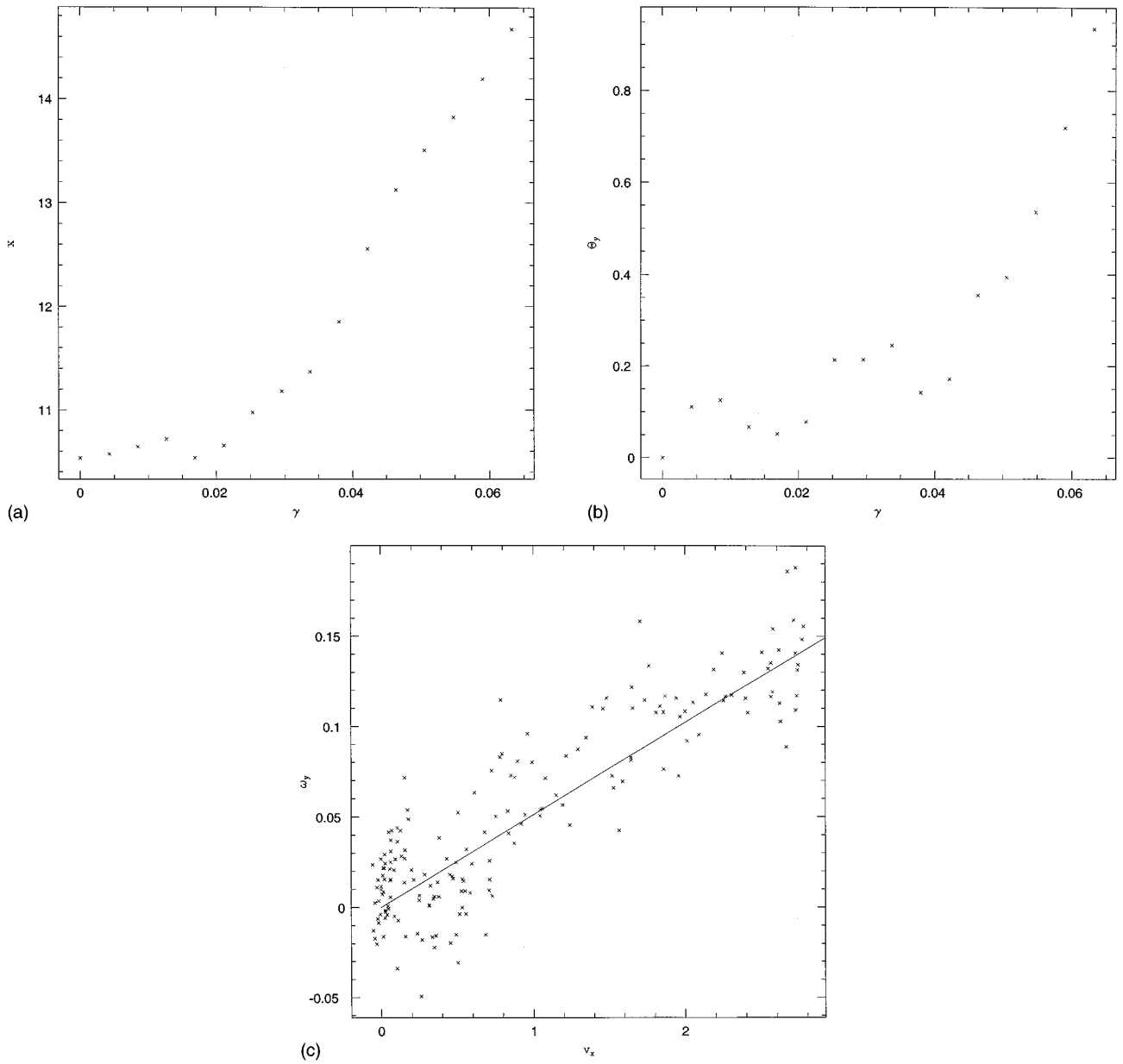

FIG. 10. (a) The x coordinate of the center of mass of the ball as a function of the applied shear rate γ. $b_m = b_s = 0.5$. (b) The angle of rotation of the ball about y axis as a function of the applied shear rate γ. $b_m = b_s = 0.5$. (c) The angular velocity of the ball vs the linear velocity of the ball. The solid line represents a linear fit. $b_m = b_s = 0.5$.

which is much larger than the radius of the ball $r = 3.5$. Obviously there is a significant slippage.

Increasing b_s increases the amount of slip. Figure 10 shows the behavior of the ball for the case when $b_s = b_m = 0.5$. In this case the effective radius, obtained from the same linear fit as before, $r_{\text{eff}} = 19.6 \pm 0.8$, is even bigger than before, which can be easily understood, if one notes that in this case the wall potential is much less corrugated than before.

The value of the shear rate γ at which the detachment occurs in our simulations is much smaller than that predicted by continuum theory [15] which suggests that the detachment ought to occur at

$$\gamma_c = 0.3 \frac{W}{R\eta} \left(\frac{W}{RK} \right)^{1/3}.$$

For the parameters in our simulation, $\gamma_c = 0.13$. From Fig. 9(a), it is obvious that the detachment starts at $\gamma \approx 0.03$. The continuum theory assumes that the detaching sphere rolls without slipping, while in our case, the significant slippage makes the detachment easier. On comparing Figs. 9(a) and 9(b), one observes that at first the ball starts sliding and only later does it begin to roll. Rotational slip, in a somewhat different context, was found in [17]—the main difference between this study and [17] is that here the rotational slip is between two solid surfaces, whereas in [17], the slip was found at the surface of a solid sphere rotating in a fluid.

VI. CONCLUSION

In this paper we have reported results of studies of several problems related to the adhesion of solids on a microscopic

level. We have shown that the predictions of the JKR theory remain valid even on a microscopic level. We have obtained excellent agreement between the JKR predictions and the results of our MD simulations without introducing any adjustable parameters. Our results have shown that introduction of roughness and/or an intervening fluid causes deviations from the JKR behavior. These deviations can be accounted for by adjusting the value of the surface energy.

We have studied adhesion hysteresis using the method of energy minimization. We have found that our system exhibits hysteresis that is unaffected by the previous history of the system. Unlike many other cases [11,12], our system does not exhibit a return-point hysteresis. We have also demonstrated that the hysteresis loops centered around different values of the central displacement δ have almost an identical shape, strongly suggesting that the hysteresis in our system arises from bulk effects.

Finally, we have studied the detachment of a spherical particle from a solid surface in a sheared flow. We have shown that detachment occurs via a mixture of rolling and sliding at smaller values of the shear rate than predicted by continuum theories. Continuum theories assume that the mechanism of the detachment is rolling, whereas in our simulations there is significant slip between the detaching particle and the solid surface.

ACKNOWLEDGMENTS

This work was supported by grants from NSF, NASA, NATO, the Pittsburgh Supercomputer Center, and the Center for Academic Computing at The Pennsylvania State University.

[1] H. Hertz, *Miscellaneous Papers* (Macmillan, London, 1896), p. 146.
[2] K. L. Johnson, K. Kendall, and A. D. Roberts, Proc. R. Soc. London, Ser. A **324**, 301 (1971).
[3] J. N. Israelachvili, *Intermolecular and Surface Forces* (Academic Press, London, 1991), 2nd ed.
[4] D. Tabor, J. Colloid Interface Sci. **58**, 2 (1977).
[5] R. G. Horn, J. N. Israelachvili, and F. Pribac, J. Colloid Interface Sci. **115**, 480 (1987).
[6] U. Landman, W. B. Luedtke, and F. M. Ringer, Wear **153**, 3 (1992); U. Landman, W. B. Luedtke, N. A. Burnham, and R. J. Colton, Science **248**, 454 (1990).
[7] P. A. Thompson and M. O. Robbins, Phys. Rev. Lett. **63**, 766 (1989); P. A. Thompson, W. B. Brinckerhoff, and M. O. Robbins, J. Adhesion Sci. Technol. **7**, 535 (1993); P. A. Thompson and M. O. Robbins, Science **250**, 792 (1992).
[8] G. S. Krest, B. Dünweg, and K. Kremer, Comput. Phys. Commun. **55**, 269 (1989).
[9] L. D. Landau and E. M. Lifshitz, *Theory of Elasticity* (Pergamon Press, London, 1959).
[10] M. A. Krasnosel'skii, *Systems with Hysteresis* (Springer-Verlag, Berlin, 1989).
[11] J. P. Sethna, K. Dahmen, S. Kartha, J. A. Krumhansl, B. W. Roberts, and J. D. Shore, Phys. Rev. Lett. **70**, 3347 (1993).
[12] M. P. Lilly, P. T. Finley, and R. B. Hallock, Phys. Rev. Lett. **71**, 4186 (1993); M. P. Lilly and R. B. Hallock, J. Low Temp. Phys. **101**, 385 (1995).
[13] F. Preisach, Z. Phys. **94**, 277 (1935); I. D. Mayergoyz, J. Appl. Phys. **57**, 3803 (1985).
[14] Y. L. Chen, C. A. Helm, and J. N. Israelachvili, J. Phys. Chem. **95**, 10 736 (1991).
[15] M. M. Sharma, H. Chamoun, D. S. H. Sita Rama Sarma, and R. S. Schechter, J. Colloid Interface Sci. **149**, 121 (1992); M. Soltani, G. Ahmadi, R. G. Bayer, and M. A. Gaynes, J. Adhesion Sci. Technol. **9**, 453 (1995); S. K. Das, R. S. Schechter, and M. M. Sharma, J. Colloid Interface Sci. **164**, 63 (1994).
[16] M. R. King and D. T. Leighton, Jr., Phys. Fluids **9**, 1248 (1997).
[17] M. Vergeles, P. Keblinski, J. Koplik, and J. R. Banavar, Phys. Rev. Lett. **75**, 232 (1995); Phys. Rev. E **53**, 4852 (1996).